A 6500-YR PALEOENVIRONMENTAL RECONSTRUCTION OF NO MAN'S LAND SINK, ABACO ISLAND, A LARGE INLAND LAKE IN THE NORTHERN BAHAMAS

A Thesis

by

GERHARD EMIL MAALE IV

Submitted to the Office of Graduate and Professional Studies of
Texas A&M University
in partial fulfillment of the requirements for the degree of

MASTER OF MARINE RESOURCE MANAGEMENT

Chair of Committee,	Peter van Hengstum
Committee Members,	Tim Dellapenna
	Karl Kaiser
Head of Department,	Kyeong Park

May 2017

Major Subject: Marine Resources Management

ABSTRACT

No Man's Land Sink is one of the largest inland lakes on the Little Bahama Bank in the northern Bahamas, so its paleoenvironmental history may provide insight into how the regional hydroclimate and groundwater systems developed over the Holocene. In its modern state, the site is shallow, brackish (20.6 psu), 170 m in diameter, and located ~700 m from the coastline. Prior to 6400 Cal yrs BP, the accumulation of peat deposits and no aquatic invertebrates (e.g., ostracodes, foraminifera, aquatic mollusks) indicate that the site was a terrestrial ecosystem. However, the site transitioned into a subaqueous freshwater environment at 6400 Cal yrs BP, when the site became palustrine-lacustrine environment until 4200 Cal yrs BP. During this time, widespread palustrine-lacustrine carbonate deposition and the appearance of freshwater to low mesohaline microfossils indicates a likely oligohaline environment in the sinkhole (charophytes, ostracodes: *Candona annae, Cypridopsis vidua,* foraminifera: *Helenina davescottensis,* mollusks: *Planorbis, Hydrobia*). A salinity increase at 4200 Cal yrs BP is inferred from the appearance of the ostracode *Cyprideis americana* that typically prefers salinities exceeding 10 psu, and deposition of laminated microbial mats. Thereafter, an organic-rich, algal sapropel unit (56.9% bulk organic matter) accumulated that was devoid of any microfossils or mollusks. This unit suggests that the lake hosted a stratified water column, where surface waters supported phytoplankton primary productivity and corrosive or anoxic bottom water conditions hampered microfossil growth or precluded their preservation. The transition to the modern environment (~20 psu) at 2600 cal yrs BP is characterized by diversification of brackish ostracodes (*Aurila floridana, Dolerocypria inopinata, and Hemicyprideis setipunctata*), foraminifera (*Elphidium* spp., *Ammonia beccarii, Triloculina oblonga*) and mollusks (*Anomalocardia, Cerithidea*). Over the middle to late Holocene, No Man's Land has experienced abrupt salinity increases that are most likely driven by southern migration of the Intertropical Convergence Zone, hurricane-induced mixing and salinization of the topmost section of

the coastal aquifer, and shoreline migration and groundwater-level rise in response to Holocene sea-level rise.

CONTRIBUTORS AND FUNDING SOURCES

I want to thank everyone involved with helping me complete this thesis. Specifically, I would like to thank Dr. Pete van Hengstum for providing me with the project, serving as my committee chair and helping with every aspect of this project. I would like to thank Drs. Tim Dellapenna and Karl Kaiser for serving on my committee, and Dr. Anja Schulze for assistance with scanning electron microscopy. I would also like to thank Tyler Winkler, Richard Sullivan and Dr. Jeff Donnelly (Woods Hole Oceanographic Institution) for helping me procure the field data, and Tessa Bittick for reading countless revisions of this thesis. This research was supported by John W. Hess Student Research Grant in Karst Sciences from the *Geologic Society of America* and an award from the Marine Geology and Geophysics Program at the National Sciences Foundation (awards: OCE-1519578, OCE-1356708). Field support provided by Nancy and Michael Albury, Friends of the Environment, and the Bahamas National Trust.

TABLE OF CONTENTS

Page

LIST OF FIGURES

Page

LIST OF TABLES

Page

1. INTRODUCTION

The northwestern Caribbean region is dominated by islands on low-lying carbonate platforms, and the paleo environmental history of these islands provides important clues for understanding regional millennial-scale climate variability in the tropical North Atlantic. The stratigraphic variability in coastal lakes, inland saline ponds, coastal lagoons, and marshes is often examined for evidence of regional environmental change (e.g., sea-level change, precipitation variability)(Dix et al., 1999). However, inland sinkholes and blue holes are another basin that can preserve paleoclimate records (Crotty and Teeter, 1984; Kjellmark, 1996; Teeter, 1989; Zarikian et al., 2005). It is typically thought that blueholes and sinkholes develop from the long-term dissolution of limestone bedrock in the subsurface, with subsequent collapse events providing subaerial exposure of circular depressions in the landscape (Mylroie et al., 1995). This thesis will examine paleoenvironmental change in a large sinkhole in the northern Bahamas (Abaco Island) and the possible roles of Holocene sea-level rise, coastal groundwater, and meridional migrations of the Intertropical Convergence Zone in driving long-term environmental change.

Coastal groundwater in the phreatic zone (saturated zone) on karst landscapes is typically divided into two zones. The upper layer is the meteoric lens (fresh to brackish water), which buoyantly floats on the lower saline groundwater (Glunk et al., 2011). These two layers are sharply divided by a halocline further inland, but towards the coast the boundary between the two layers destabilizes into a thicker mixing zone (Beddows et al., 2007). On millennial timescales, the water quality of the upper meteoric lens is usually in dynamic equilibrium with local precipitation (e.g., precipitation and evaporation), while the absolute elevation of the groundwater itself (i.e., the water table) is ultimately controlled by sea level variability (Richards et al., 1994; van Hengstum et al., 2011). For example, during periods of sea-level rise, the meteoric lens also vertically rises in the subsurface (van Hengstum et al., 2011). Given the high permeability and high porosity of karst landscapes, inland sinkholes are typically open systems because

the antecedent geology allows for the uninhibited circulation of groundwater (Zarikian et al., 2005). By assessing how groundwater elevation and salinity of the meteoric lens changed through time, one could potentially document the effects of regional hydrologic variability and sea-level rise on coastal carbonate aquifers.

In general, precipitation in the Caribbean region is driven by many ocean and atmospheric forces on seasonal and annual timescales (Jury et al., 2007), but on Holocene timescales, it is thought that regional precipitation has varied in response to southern migration of the Intertropical Convergence Zone (McGee et al., 2014) (Haug et al., 2001; Hodell et al., 1991). The ITCZ is a latitudinal zone of low pressure at the Equator demarcating the boundary between two adjacent Hadley Cells, associated with strong atmospheric convection and cloud cover (Orem et al., 1986). This area of low pressure is where humid trade winds converge on the warmest regions of the ocean (Linsley et al., 1994a). It is associated with increased precipitation, and is typically thought of as the meteorological equator. In general, the ITCZ seasonally migrates, where it occupies its most northern (southern) position in July (January) (Linsley et al., 1994a). Small ITCZ movement variations, of even a few degrees, can significantly affect rainfall regional distribution in the tropics (Linsley et al., 1994b). Over the Holocene, the ITCZ has migrated southward, likely due to orbital forcing (Haug et al., 2001; Hodell et al., 1991). However, current numerical models predict very little change in ITCZ position over the Holocene (e.g. 10°42.73N, 65°10.18W) (McGee et al., 2014), yet paleohydrological studies from across the Caribbean document significant periods of aridity versus deluge.

1.1 Research Questions

This thesis will attempt to answer the following questions:

1. What is the paleoenvironmental history of No Man's Land Sink, a large sinkhole on Abaco Island in the northern Bahamas?

2. Do the microfossils (i.e., ostracodes, foraminifera) record any changes to the salinity of the groundwater that is flooding the sinkhole (e.g., meteoric lens) over millennial timescales?
3. If salinity variations can be determined, what ocean-atmospheric factors forced these paleosalinity changes?

2. LITERATURE REVIEW

2.1 Caribbean Climate Variability

There has been considerable paleoenvironmental research examining millennial-scale precipitation throughout the Caribbean region, however, fewer studies have been completed in the northern Caribbean. In Laguna de la Leche in Cuba, sediment cores were analyzed for pollen, calcareous microfossils and geochemistry. Based on the information yielded from the core analysis, it can be inferred that at 6200 Cal yrs BP the lake was dry and it became flooded at 4200 Cal yrs BP by rising groundwater from regional sea-level rise (Peros et al., 2007). In another study from Cuba, cores were taken from the coastal lagoons Punta de Cartas and Playa Bailen and analyzed for foraminifera, bulk organic matter, and trace metal abundance via x-ray fluorescence scanning (Gregory et al., 2015). Four distinct microfossil biofacies, and decreasing abundance of terrestrially-derived trace metals, were observed that indicated increasingly marine conditions in the lagoon and regional aridity towards the present (Gregory et al., 2015). Gypsum crystals were also observed in the stratigraphy from ~2600 to 3300 Cal yrs BP, which are perhaps suggestive of a regional arid period. From 1400 to 1100 Cal yrs BP, observed microfossils also indicate higher salinity in the lagoons, which also suggest regional aridity, and these aridity periods were attributed to a southerly shifting Intertropical Convergence Zone (Gregory et al., 2015). The oxygen isotopic variability of speleothems provides an alternate hydroclimate proxy, and Fensterer et al. (2013) compiled a 12,500-year record of precipitation change from Cuba that also indicates long-term precipitation change over the Holocene related to southward ITCZ migration. On San Salvador Island in the Bahamas, ostracodes have been used to examine the paleosalinity variation of several inland sinkholes during the mid-Holocene, and these salinity variations were previously attributed to regional sea-level variability (Teeter, 1995). On Lee Stocking Island, paleoenvironmental change in a coastal pond over the last 1500-years was impacted by both sea-level variability and regional climate change (Dix et al., 1999). On nearby Andros Island, a study of late

Holocene climate change was completed on Church's Blue Hole where pollen was used as paleoenvironmental proxy (Kjellmark, 1996). The pollen record indicated a period of aridity in the northern Bahamas from 3200 to 1500 yrs BP, which was based on the dominance of arid-adapted shrubs on the regional landscape. A paleoclimate reconstruction based on the oxygen isotopic variability in ostracode shells from Haiti also noted the period of Caribbean aridity at the same time (Hodell et al., 1991). More recently, a period of intense hurricane activity was documented in Puerto Rico (Donnelly and Woodruff, 2007) and the northern Bahamas (van Hengstum et al., 2016) from 2600 to 1000 Cal yrs BP that has been attributed to a more northern position of the ITCZ (van Hengstum et al., 2016).

Considerable paleoenvironmental research has been completed on Abaco Island to understand landscape, ecological, and sea-level variability over the Holocene. For example, sediment cores collected from a coastal sinkhole on the eastern shoreline indicate that the sinkhole was likely a freshwater marsh or terrestrial environment prior to 1200 years ago, and thereafter become an anchialine environment when it was flooded by regional sea-level rise (Kovacs et al., 2013). Elsewhere on Abaco Island, an inland sinkhole (Slayton, 2010a) documented 8400 years of regional vegetation change through the preserved pollen, and an increase in pine on the landscape in the last ~1000 years (Slayton, 2010b). Interestingly, earlier in the Holocene Abaco Island hosted reptile-dominated terrestrial ecosystems (Hastings et al., 2014), which also disappeared at 1000 Cal yrs BP. Perhaps, the hydrographic variability in a large inland lake can better place these regional and local environmental changes into a context of regional precipitation change.

2.2 Bahamian Inland Lakes and Ostracodes

Considerable research has been conducted to understand environmental processes, past and present, in Bahamian sinkholes, blueholes, and inland saline lakes (Dix et al., 1999; Park et al., 2009). Since lakes on carbonate platforms can be formed by a variety of hydrologic processes, (Boush et al., 2014) describes a model for the

formation of Bahamian lake environments after analysis of 52 lakes. In short, the model describes lakes that form in response to carbonate dune formation, coastal geomorphological changes, and subsequent carbonate platform flooding by sea-level rise (termed ‘constructional lakes’); other lakes that form from groundwater and limestone collapse processes (termed ‘destructional lakes’); and some lakes are the result of an interaction between the two (Boush et al., 2014).

One of the most important geomorphologic characteristics influencing lake hydrology is if the lake is connected to the ocean via conduits or caves, if the lake behaves as an open system with the local coastal aquifer, or if the lake is isolated from hydrographic circulation between either the ocean and coastal aquifer (Boush et al., 2014). The salinity of destructional inland lakes that are connected to the ocean via caves are modulated by coastal oceanographic conditions. In contrast, destructional inland lakes connected with the coastal aquifer likely have stratified water columns, with the upper meteoric lens divided from the saline groundwater below by a halocline or mixing zone [(example: Church’s Bluehole in Andros, (Kjellmark et al., 1996)]. Lastly, the salinity in lakes that are isolated from both groundwater flow and oceanic conditions are dependent upon local evaporation and precipitation, both of which will be influenced by climate change on millennial and centennial timescales.

One of the main environmental indicators used to understand Bahamian lake evolution is benthic ostracodes because their ecology is strongly linked to lake salinity, but also other environmental factors (Teeter et al., 1986; Teeter, 1995; Park and Trubee, 2008; Michelson and Park, 2011, 2012; Bowles, 2013). Ostracodes are freshwater to marine crustaceans that produce a simple carapace, or shell, of calcium carbonate with two valves that is preserved in the sediment as a microfossil after the crustacean dies. The shells have excellent preservation in the fossil record, and so they are very useful as paleoenvironmental proxies (Alonso-Zarza and Tanner, 2009). They are abundant within Bahamian terrestrial aquatic systems (Teeter, 1995), and certain species are indicative of specific environmental conditions. Previous studies have established the ecological salinity tolerances for several ostracodes species. Based on cores from Salt Pond and

Watlings Blue Hole on San Salvador Island, *Hemicyprideis setipunctata* commonly lives in salinity rages of 25-35 psu, *Cyprideis americana* lives in salinity rages of 10 to 98.5 psu, *Dolerocypria inopinata* in salinity rages of 10.8 to 98.5 psu (Teeter, 1995), *Limnocythere floridensis* can survive in salinity ranges from 44 to 100 psu (Teeter, 1980) but also oligohaline conditions (Teeter, 1980) *Candona annae* and *Cypridopsis vidua* are commonly found in freshwater conditions (Teeter, 1995), and *Aurila floridana* lives in more marine conditions of 30 to 40 psu (Teeter, 1995). Storrs lake on San Salvador in the Bahamas has assemblages of *Hemicyprideis setipunctata* and *Cyprideis americana*(Sipahioglu, 2008) , and benthos of this inland saline lake is characterized by abundant microbialites (Sipahioglu, 2008). Recently, Park and Trubee (2008) list the salinities of most Bahamian ostracods found in the Bahamas, and scanning electron micrographs are available to identify many common species of Bahamian ostracodes (Furtos, 1936; Krutak, 1971; Michelson, 2012; Pérez et al., 2010; Teeter, 1980; Teeter, 1995; Zarikian et al., 2005)

3. STUDY SITE

The Bahamas are a group of island carbonate banks located in the tropical North Atlantic Ocean. There are roughly 700 cays (pronounced ‘keys’) that make up these islands spreading over 14,400 square kilometers (Correll, 1979). The carbonate sediments that built the Bahamian archipelago likely began deposition in the late Jurassic (Mullins and Lynts, 1977), and the surficial geology is now characterized by a matured karstified landscape with abundant sinkholes and blueholes (Mylroie et al., 1995). No Man’s Land is likely an ancient sinkhole that is located 700 m from the shoreline on the western coast of Abaco Island in the Northern Bahamas (Figure 1). Despite being the 2nd largest sinkhole on the island (170 m in diameter), it is relatively shallow (3 meters deep) and currently flooded with brackish groundwater (20.6 psu). The sinkhole itself is surrounded by typical northern Bahamian pine forests.

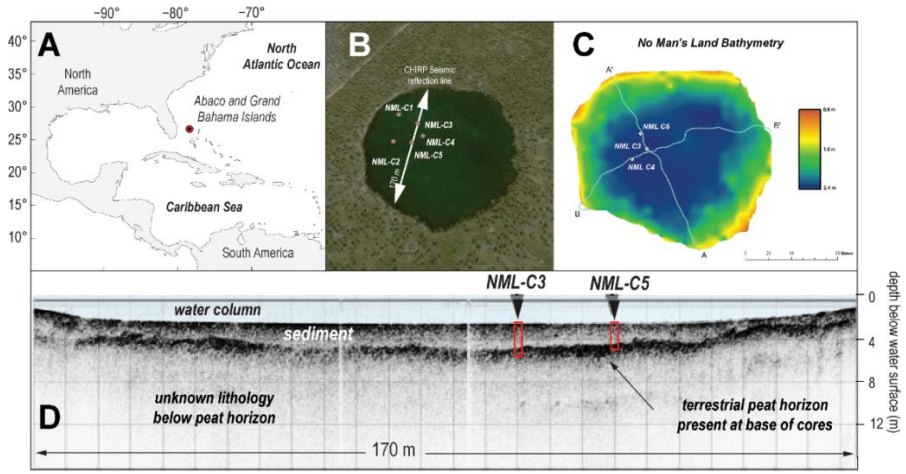

Figure 1. Schematic of NML sink. **(A)** Location of Great Abaco Island in the tropical North Atlantic Ocean; **(B)** aerial photograph of No Man's Land Sink, including the location of the sediment cores and seismic reflection profile; **(C)** bathymetric map of sinkhole; **(D)** seismic reflection profile across the sinkhole, indicating prominent subsurface reflector (terrestrial peat) and locations of core 3 and core 5

4. METHODS

Five push cores were collected from No Man's Land sinkhole in 2014 (Figure 1A). A seismic reflection survey was completed with an Edgetech 424 CHIRP, to image the subbottom stratigraphy (Figure 1D). The Edgetech uses a sweep signal of varying frequencies (4-24 khz) of sound waves to penetrate the sediments on the sinkhole floor and generate a subsurface profile (Quinn et al., 1998). Two-way travel time was converted to depth in meters using a water velocity of 1500 m/s. This imagery was then used to determine the ideal locations to collect five push cores (Figure 1B), which ranged in length from 70 to 120 cm. The cores terminated on a dense acoustic reflector, which the subsequent sediment cores revealed to be terrestrial peat deposit (Figure 1D, see Results). Depths acquired during the seismic reflection survey were used to generate a bathymetric map (Figure 1C). Transects, using the Edgetech 424 Chirp sub-bottom profiler, were run both vertically and horizontally across No Man's Sink. Combined with a GPS, this system records the latitude, longitude, and depth.

After collection, the five sediment cores were transported back to the laboratory where they were split lengthwise, visually described, photographed, x-radiographed to image sediment density, and subsequently stored at 4°C until further analyzed. Core lithologic descriptions generally follow Schnurrenberger et al. (Schnurrenberger et al., 2003). The variability in the coarse sediment fraction was analyzed using the Sieve-first Loss-on-Ignition (Sieve-first LOI) procedure (van Hengstum et al., 2016). Contiguous 1-cm sediment sub-samples with an initial volume of 2.5 cm^3 were first sieved over a 63-μm sieve and dried for 12 hours in a drying oven at 60˚C, and weighed to determine the original sediment mass. After they were dried and re-weighed, samples were ignited for 4.5 hours at 550˚C in a muffle furnace to remove organic matter from the sediment samples and concentrate the remaining mineral residue. The variability in coarse sediment was then expressed as mass per unit volume ($D_{>63\ um}$ mg cm^{-3}). A classic LOI procedure was then completed to determine the downcore variability in bulk organic matter (Dean Jr, 1974; Heiri et al., 2001). New sub-samples were taken from the core at

contiguous 1 cm intervals and first weighed, then desiccated overnight at 60˚C, and reweighed to determine percent moisture by mass lost. Dried sediment samples were then ignited at 550˚C for 4.5 hours, and re-weighed when they were cool to determine the percentage of bulk organic matter.

Previous research indicates that abundant microfossils (e.g., foraminifera and ostracodes) are present in Bahamian terrestrial sinkholes, which can be used to document groundwater salinity changes on millennial timescales (Teeter, 1989). The two longest cores (i.e., NML-C4, NML-C5) were selected for detailed microfossil analysis, and separate sediment samples were processed for benthic foraminifera and ostracodes. NML-C4 was sampled for foraminifera and ostracodes at 2.5 cm intervals, whereas, NML-C5 was sampled at 10 cm intervals. For foraminiferal analysis, sediment samples were wet sieved over a 63 µm sieve and the remaining sediment residue was first inspected for fragile, organic walled microfossils (e.g., testate amoebae, agglutinated foraminifera). The remaining sediment residues were then dried overnight and foraminiferal tests were picked and mounted on micropaleontological slides for taxonomic identification and enumeration. However, from 80 cm to 72 cm in NML-C4 and 112 cm to 102 cm in NML-C5 were sieved using a 45 µm sieve to examine for the presence of the small foraminiferan *Helenina davescottensis*. For ostracode analysis, another sediment sample was wet sieved over a 125 µm sieve, dried overnight, and ostracode valves were picked and mounted on micropaleontological slides for further taxonomic identification and enumeration. Where possible, at least 150 foraminiferal tests and ostracode valves were picked from the samples. No attempt was made to differentiate ostracode gender or valve (left vs. right). However, given the low diversity of both ostracode and foraminifera in the sediment samples, significant paleoenvironmental information can be obtained with the observed microfossils. Next, taxonomic identifications were verified with Hitachi TM3000 scanning electron microscope and available taxonomic references from the literature (Figure 4)(Furtos, 1936; Krutak, 1971; Michelson, 2012; Pérez et al., 2010; Teeter, 1980; Teeter, 1995; Zarikian et al., 2005).

Fractional (or relative) abundance (Beddows et al.) was then calculated separately for ostracodes and foraminifera, where *n* is the total number of individuals in a sample, and x_i is the total number of individuals of a specific species observed in a sample:

$$Fi = \left(\frac{xi}{n}\right) * 100$$

The relative abundances were plotted against the core logs in the freeware program *C2* (https://www.staff.ncl.ac.uk/stephen.juggins/software/C2Home.htm)(Figure 3). Lastly, the ostracode fractional abundance data was then used for biofacies analysis. Downcore biofacies were identified using Q-mode cluster analysis with a Bray-Curtis similarity distance metric in the freeware program *PAST* (http://folk.uio.no/ohammer/past/).

To establish chronological control, organic material from the sediment cores was submitted for radiocarbon dating (Table 1) at the National Ocean Sciences Accelerator Mass Spectrometry Facility (NOSAMS) at Woods Hole Oceanographic Institution (Zarikian et al., 2005). Wood fragments were submitted for radiocarbon dating when possible, as they are in equilibrium with secular variations in atmospheric radiocarbon. Problematically, wood fragments were not always present at important stratigraphic horizons, so bulk organic material was instead submitted for radiocarbon dating. The bulk organic matter submitted was gelatinous sapropel produced by aquatic algae. To help characterize the possible hardwater effect that was imparted on the bulk organic matter generated by algae living in groundwater, the conventional ^{14}C age of the twig sample from NML-C5 24 to 25 cm (3090 ± 20 conventional years ago) was subtracted from the bulk organic sample of NML-C4 46 to 47 cm (3730 ± 20 conventional years ago). It is assumed that these samples were deposited at a similar time given the small size of the basin and that they are located just below the same salient stratigraphic contact. This resultant hardwater effect (640 ± 40 conventional years ago) was subtracted from the conventional ages obtained on other bulk organic matter samples (Zarikian et al., 2005). It assumes that this hardwater effect has been constant throughout

time. Thereafter, all radiocarbon ages were converted into calibrated years before present (Cal yrs BP) using IntCal13 (Reimer et al., 2013) in Calib 7.1 (http://calib.qub.ac.uk/calib/).

5. RESULTS

Five different sedimentary units were present in the uppermost stratigraphy of No Man's Land, most of which could be correlated in the subsurface between the cores. Based on the oldest radiocarbon date, the recovered successions were deposited since the middle Holocene, or 6500 calibrated years before present (Cal yrs BP).

Table 1. Radiocarbon ages obtained on organic material from the sediment cores.

Core	Core depth (cm)	Material dated	$F^{14}C$	Conventional ^{14}C age	Hardwater Effect Removed (640 ± 40)	$\delta^{13}C$ (‰)	1σ calendar ages in yrs. B_{1950} (probability)	2s calendar ages in yrs. B_{1950} (probability)	Highest probability 1σ age
C2	14.5 to 15.5	pine cone fragment	0.6068 ± 0.0020	4010 ± 25		-26.08	4437 - 4449 (0.190)	**4423 - 4524 (1.000)**	4490 ± 30
							4466 - 4517 (0.810)		
C3	17 to 18	bulk organics	0.6749 ± 0.0015	3160 ± 20	2520 ± 60	-21.97	**2494 - 2598 (0.544)**	2380 - 2394 (0.016)	**2540 ± 50**
							2610 - 2639 (0.151)	2402 - 2413 (0.010)	
							2681 - 2741 (0.305)	2424 - 2751 (0.974)	
C3	36 to 37	bulk organics	0.6401 ± 0.0018	3580 ± 25	2940 ± 65	-25.38	**2995 - 3180 (0.977)**	2888 - 2907 (0.013)	**3090 ± 100**
							3200 - 3205 (0.023)	**2922 - 3254 (0.957)**	
								3294 - 3328 (0.029)	
C3	57 to 58	stems	0.5844 ± 0.0015	4310 ± 20	3670 ± 60	-25.95	**3920 - 4086 (1.000)**	**3840 - 4153 (1.000)**	**4000 ± 83**
C4	19.5 to 20	bulk organics	N/M	3150 ± 40	2510 ± 60	N/M	**2492 - 2602 (0.554)**	2379 - 2395 (0.019)	**2550 ± 60**
							2607 - 2641 (0.167)	2400 - 2414 (0.018)	
							2678 - 2737 (0.279)	2421 - 2747 (0.963)	
C4	38.5 to 39	bulk organics	0.6173 ± 0.0016	3880 ± 20	3240 ± 60	-24.83	**3396 - 3509 (0.826)**	**3357 - 3608 (1.000)**	**3450 ± 60**
							3531 - 3556 (0.174)		
C4	46 to 47	bulk organics	0.6287 ± 0.0015	3730 ± 20	3090 ± 60	-22.2	**3228 - 3370 (1.000)**	3084 - 3087 (0.001)	**3300 ± 70**
								3156 - 3447 (0.999)	
C4	83	bark	N/M	5660 ± 40		N/M	**6405 - 6484 (1.000)**	6319 - 6375 (0.107)	6440 ± 40
								6386 - 6539 (0.893)	
C4	99	twig	0.4717 ± 0.0020	6040 ± 35		-28.42	6805 - 6812 (0.069)	**6790 - 6979 (1.000)**	6900 ± 50
							6850 - 6942 (0.931)		
C5	24-25	twig	0.6803 ± 0.0016	3090 ± 20		-24.85	**3254 - 3293 (0.611)**	**3241 - 3364 (1.000)**	3270 ± 20
							3328 - 3356 (0.389)		
C5	39	tim	0.6205 ± 0.0019	3830 ± 25		-25.87	**4155 - 4208 (0.592)**	4103 - 4109 (0.006)	4181 ± 30
							4219 - 4250 (0.331)	**4148 - 4299 (0.924)**	
							4273 - 4283 (0.078)	4327 - 4354 (0.045)	
								4369 - 4385 (0.018)	
								4392 - 4401 (0.007)	

The basal sedimentary unit was a peat deposit (Figure 2), which sharply transitions into a carbonate mud unit that passes into a laminated carbonate mud upsection. Thereafter, a layer of sapropel accumulated before modern carbonate sand deposition was initiated. The results of Q- and R-mode cluster analysis on the relative abundance of ostracodes indicate the presence of three distinct biofacies that were dominated by different fauna, which can be linked with discrete salinity conditions (i.e., freshwater, low brackish, polyhaline). The preservation of other invertebrates (e.g., bivalves, gastropods) and microfossil remains (benthic foraminifera, charophytes) confirms the environmental assessment provided by the ostracode biofacies. The sedimentary facies, ostracode biofacies, and the timing of their deposition, are described in detail below.

5.1 Peat Facies

A peat deposit was recovered at the base of all cores except NML-C3. Based on the seismic reflection survey, the most prominent acoustic reflector observed throughout the basin in the subsurface occurred at a depth of ~1 m below the sediment-water interface. This strong acoustic reflector is the peat deposit based on the position of the peat facies in the cores (Figure 2, 3). Deposition of the peat is partially constrained by the basal radiocarbon dates in NML-C4 (83 cm), which indicate the peat deposit was accumulating prior to 6440 ± 40 Cal yrs BP (Zarikian et al., 2005). Sedimentologically, the peat is dark brown in color, and it contained 42.8 mg cm^{-3} of coarse sediment ($D_{>63\ um}$) and a mean 64.9 ± 24.9% bulk organic matter (Table 2, Figure 3). The peat did not contain mangrove roots or propagules, and was not dominated by forest macrofossils (e.g., bark, twigs, leaves, pine needles). Based on the classification of Schnurrenberger et al. (Schnurrenberger et al., 2003), this is a fragmental granular peat deposit. Some pebbles were found at the base of core 2. No microfossils or other invertebrates were present (e.g., testate amoeba, foraminifera, ostracodes).

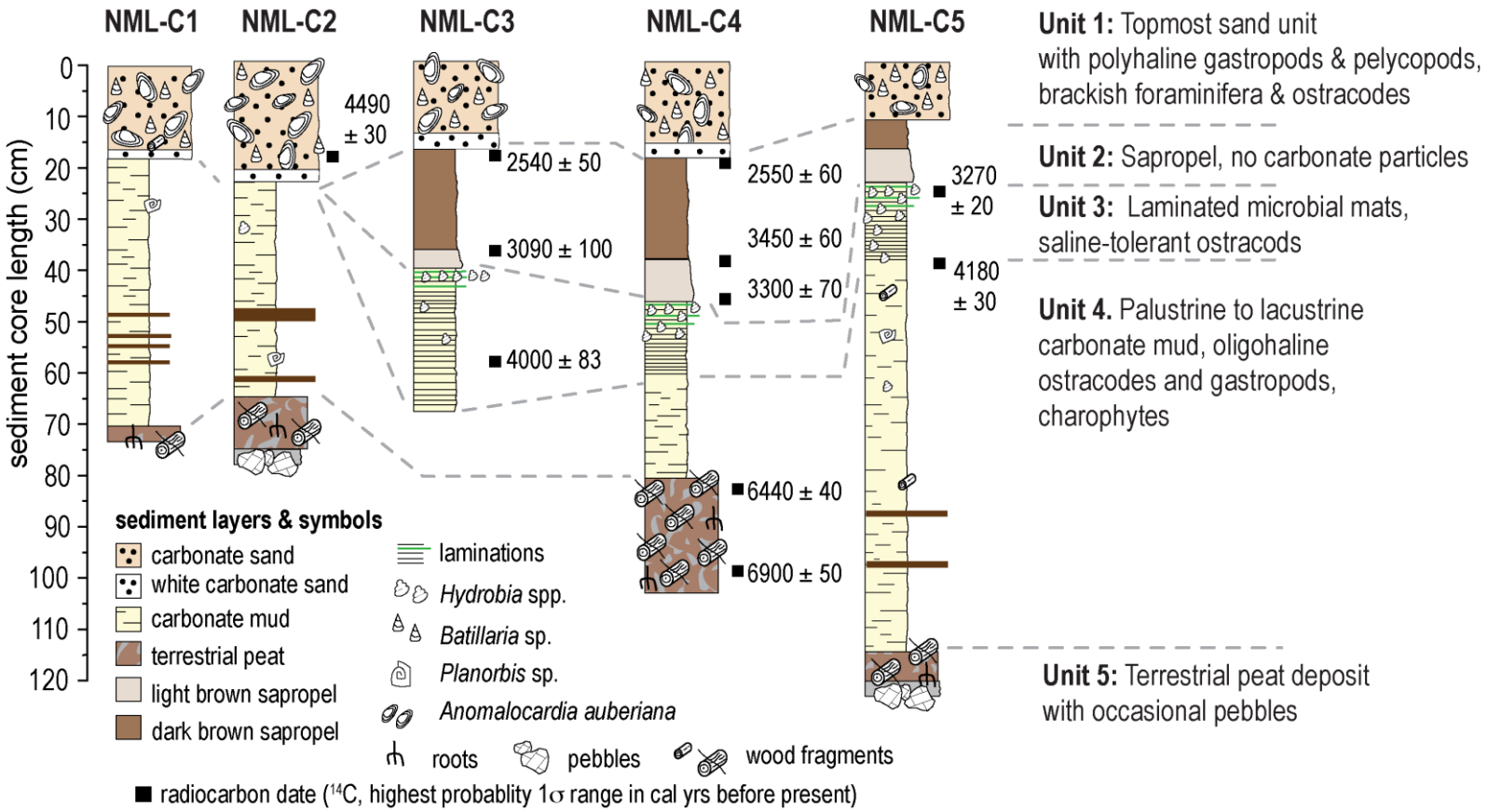

Figure 2. Correlation diagram of cores collected from No Man's Land Sink.

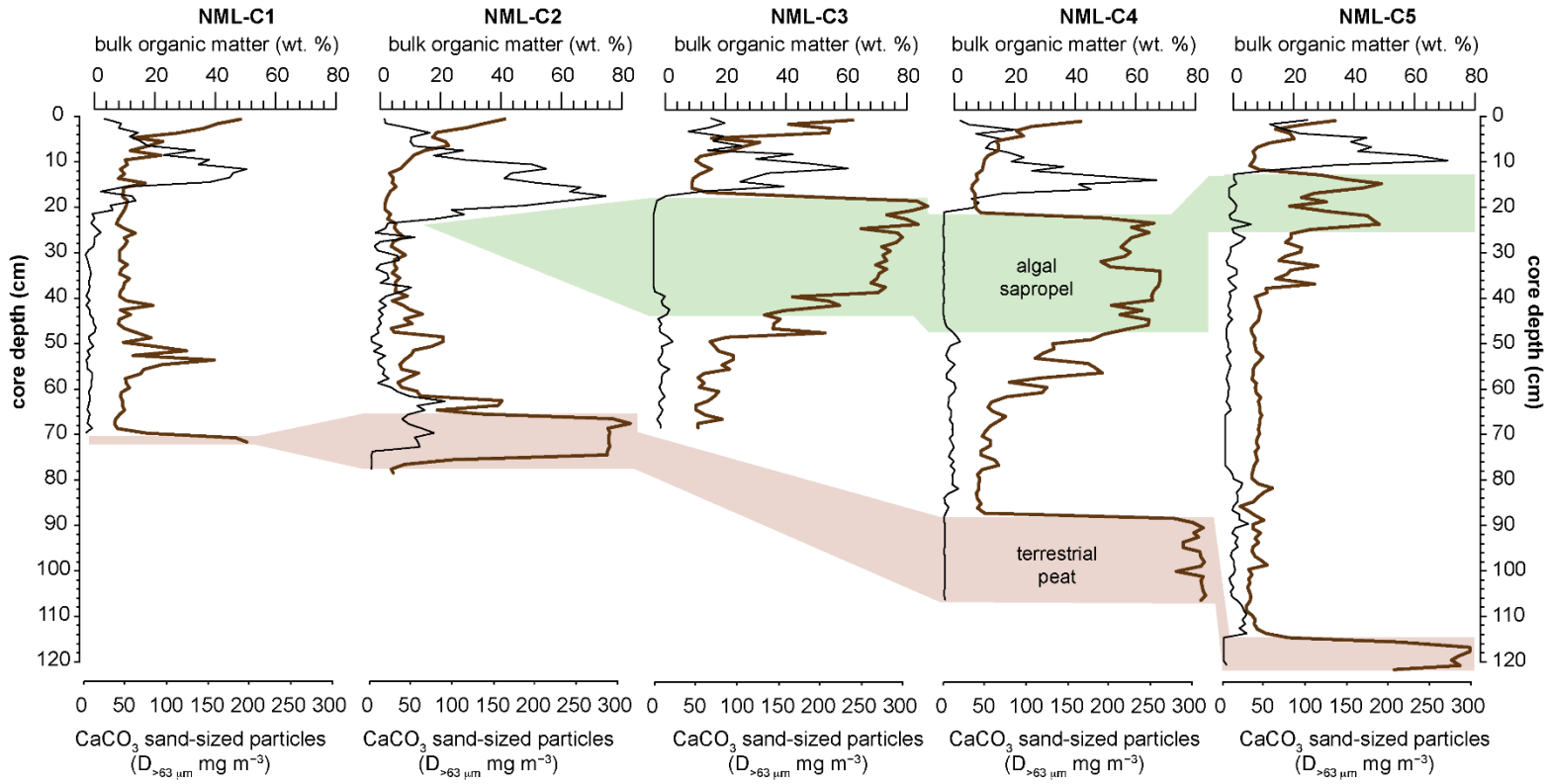

Figure 3. Bulk organic percentages and $CaCO_3$ sand-sized particles in each core.

Table 2. Average and standard deviation of bulk organic content (wt. %), mean coarse fraction content (D>63 um mg cm−3), and dominant microfossils in each of the sedimentary facies.

Facies (timeline of deposition)	Bulk Organic %	Coarse Fraction mg cm−3	Average fractional abundances of dominate ostracodes	Average fractional abundances of dominate Foraminifera
Carbonate Sand (2600 to present Cal yrs BP)	18.5 ± 14.6	114.5 ± 68.6	*Dolercypria inopinata* 10.4 ± 9.6 *Hemicytheridea setipuncta* 19.7 ± 7.1 *Aurila floridana* 55.5 ± 16.8 *Limnocythere floridensis var. rounded* 14.4 ± 7.2	*Ammonia beccarii* 63.7 ± 27.7 *Elphidium poeyanum* 6.0 ± 5.8 *Triloculina Oblonga* 26.8 ± 27.9
Sapropel (3300 to 2600 Cal yrs BP)	56.8 ± 18.8	5.8 ± 11.7	None	None
Laminated Mud (4200 to 3300 Cal yrs BP)	25.0 ± 13.3	11.0 ± 5.4	*Cyprideis americana* 18.2 ± 21.3 *Unknown sp. A* 81.6 ± 21.1	None
Carbonate Mud (6500 to 4200 Cal yrs BP)	11.6 ± 10.1	11.9 ± 12.0	*Candona annae* 25.6 ± 31 *Cypridopsis vidua* 71.7 ± 32.1 *Limnocythere floridensis var. pointed* 2.2 ± 3.4	*Helenina davescotensis* 18.2 ± 39.5
Peat (>6500 Cal yrs BP)	64.9 ± 25.0	42.8 ± 122.0	None	None

5.2 Carbonate Mud Facies

Based on the radiocarbon results, the carbonate mud facies accumulated between 6500 to 4200 Cal yrs BP. This layer was represented in all cores except NML-C3.The sediment is light brown in color with discontinuous layers and lenses of dark brown organic matter. The average organic matter content was 11.6%, with an average coarse fraction content of 12.71 mg cm^{-3}. The following species of ostracodes were dominant in this layer: *Limnocythere floridensis* var. pointed, *Candona annae*, and *Cypridopsis vidua.* NML-C5 also had an additional ostracode species located in this facies, *Limnocythere floridensis* var. pointed. Only one species of benthic foraminifera was present in the carbonate mud layer, *Helenina davescottensis*, and it is only present in NML-C4 from 70 to 80 cm (Fig. 5, 7). There was one species of foraminifera located in the carbonate mud layer of NML-C4 only. It is the newly described species known as, *Helenina davescottensis*. There was also two gastropod species present in this layer (*Planorbis, Hydrobia).*

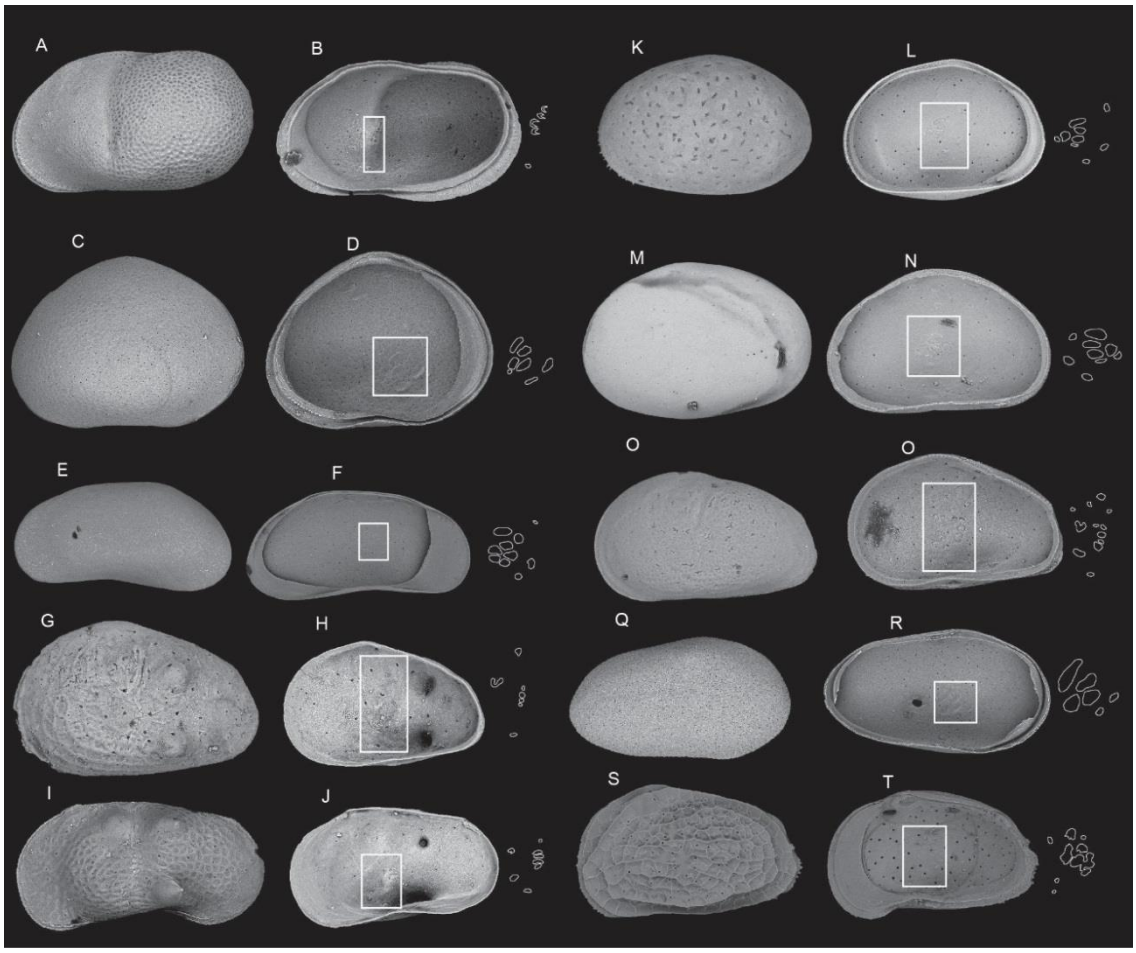

Figure 4. Scanning electron micrographs of recovered ostracodes (external and internal views, with enlarged line drawings of the adductor muscle scars outlined on right). **A, B**: *Cytheridella ilosvayi* (Daday), **C, D**: *Cypridopsis vidua* (Müller), **E, F**: *Candona annae* (Mehes), **G, H**: *Limnocythere floridensis* (Keyser), var. rounded, **I, J**: *Limnocythere floridensis* (Keyser), var. pointed, **K, L**: *Hemicyprideis setipunctata* (Brady), **M, N**: Unknown sp. (c.f.,*Hemicyprideis setipunctata?*), **O, P**: *Cyprideis americana* (Sharpe), **Q, R**: *Dolerocypria inopinata* (Klie), **S, T**: *Aurila floridensis* (Keyser).

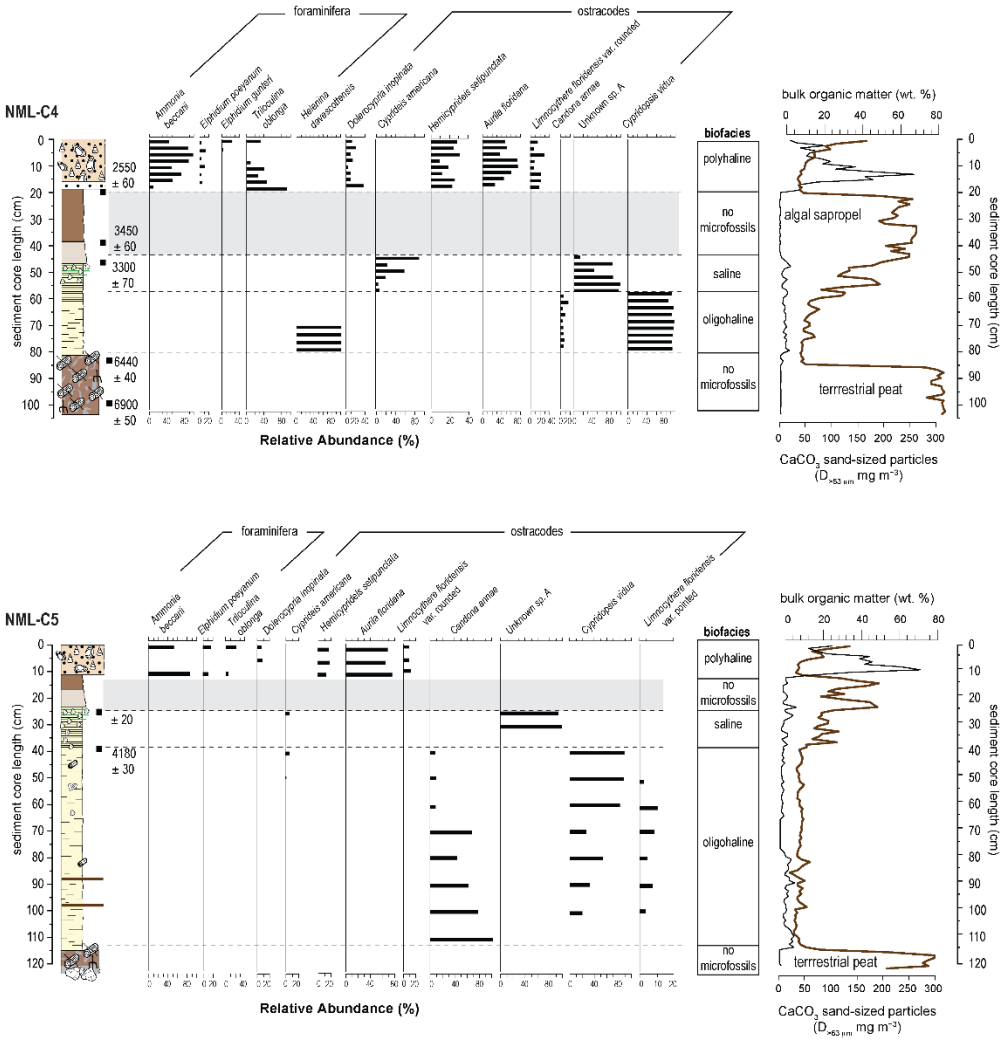

Figure 5. The relative abundance of dominant foraminifera and ostracodes in NML-C4 and NML-C5. This also shows textural variability and biofacies determined with Q-mode cluster analysis.

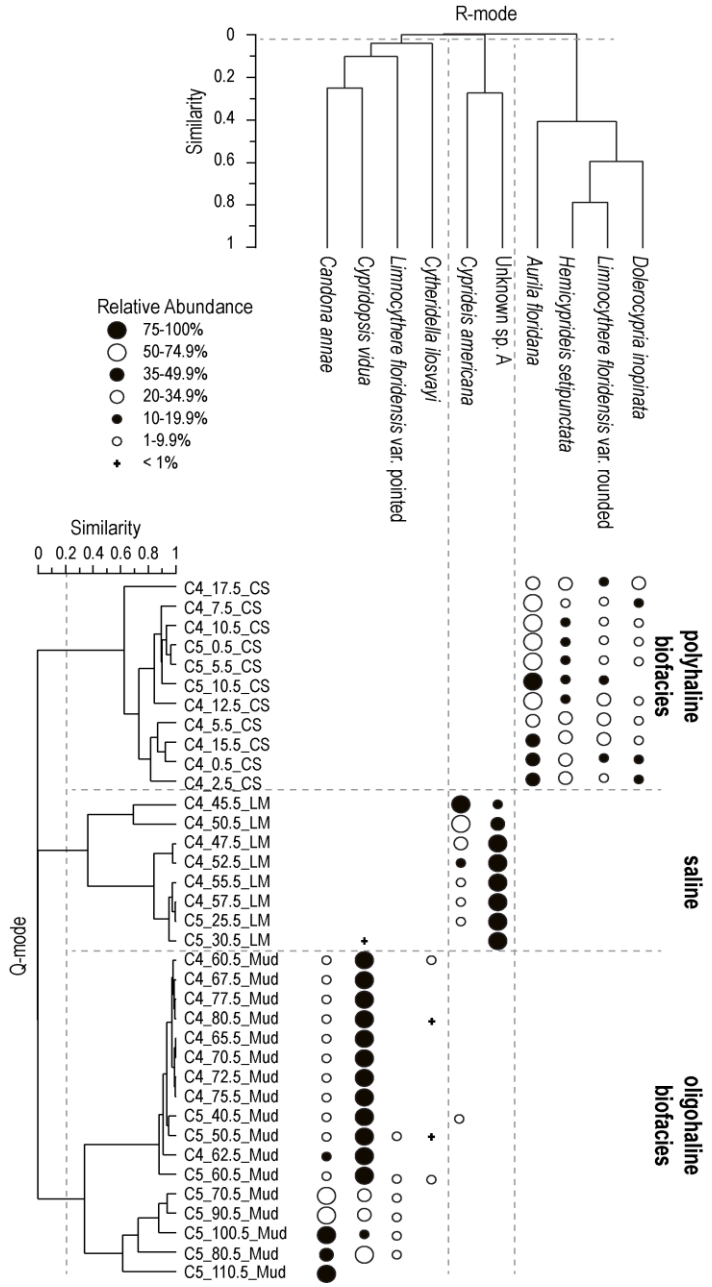

Figure 6. Dendrogram and cluster analysis. This was produced using paired group cluster analysis (Q- and R-mode) and a Bray-Curtis similarity distance co-efficient to identify ostracode biofacies in NML-C4 and NML-C5. Q mode shows the similarity of each sample to one another, while R mode indicates how prevalent different species of ostracodes occur with one another.

Previous studies indicate that *Cypridopsis vidua* and *Candona annae* prefer low salinity environments, fresh to oligohaline (0 to 3.5 psu) (Teeter, 1995; Zarikian et al., 2005). In addition, *Limnocythere floridensis* var. rounded was also found in this layer, but only in NML-C5. This variant of *Limnocythere floridensis* had notably rounded nodes and a more rounded external morphology than *Limnocythere floridensis* var. pointed, and the former was only present in this biofacies. Given the distinctive morphological differences, these individuals were enumerated separately in this study. Teeter (1995) indicates that *Limnocythere floridensis* colonizes freshwater settings in inland lakes and sinkholes on San Salvador Island (Bahamas). However, Teeter (Teeter, 1980) images individuals of *L. floridensis* that appear to have both the 'pointed' and 'rounded' morphology from Pleistocene-aged sediments in Florida (Teeter, 1980, plate 6, figs. 1-6), and interpreted their dominance to be indicative of mesohaline conditions. No testate amoeba (van Hengstum et al., 2008), which are freshwater microfossiles, were observed in the carbonate mud layer. However gyrogonites of charophytes were observed throughout the facies, which are the reproductive parts of a freshwater to slightly brackish macrophyte (Soulié-Märsche, 2008).

5.3 Laminated Carbonate Mud Facies

The laminated carbonate mud facies was deposited between 4200 to 3300 Cal yrs BP. It was present in all cores except NML-C1 and NML-C2. This facies was laminated, and laminations varied in color between grey, green, dark brown and even purple. This layer had an average organic matter content of 25%, and coarse fraction content of 11.9 mg cm^{-3}. In cores NML-C4 and NML-C5, the ostracodes *Cyprideis americana* and *Unknown species A* were dominant. Based results from elsewhere, *C. americana* can tolerate salinity ranges from 10.8 to 98.5 psu (Teeter, 1995). The muscle scars from *Unknown sp. A* are very similar to the muscle scars from *H. setipunctata,* however there are no sieve pores on *Unknown sp. A* like on the carapace of *H. setipunctata*. No species of foraminifera were present, but small gastropods (cf. *Hydrobia?*) were abundant and

gyrogonites of charophytes present. The ostracode *C. americana* found within this layer right before the sapropel zone contained very heavy 'pitting' on the carapace.

5.4 Sapropel Facies

The sapropel facies was deposited between 3300 to 2600 Cal yrs BP, and it had two distinctive layers: a lower lighter brown layer and an upper darker brown layer. By definition, sapropel is an aquatic ooze that contains over 50% bulk organic matter that is rich in amorphous or very fine grained organic matter particles (Schnurrenberger et al., 2003). The sapropel facies from No Man's Land had the highest organic matter content (mean 56.8%) with a low content of coarse sediment particles (5.8 mg cm^{-3}). The sediment was comprised of amorphous organic matter particles, and terrestrial plant macrofossils were not present. It had the physical appearance of the algal sapropel that has been accumulating in Mangrove Lake in Bermuda over the middle to late Holocene, which is a shallow, anoxic inland saline lake in Bermuda (Orem et al., 1986). However, anoxic conditions are not a pre-requisite for the accumulations of algal sapropels. For example, Kemp's Bay Bluehole on Andros Island is brackish and is presently accumulating an algal sapropel. No microfossils or macrofossils were present in this layer. In the uppermost darker brown layer, vertical burrows (2-3 cm) were present that were likely derived from bivalves associated with the upper most facies (carbonate sand facies). Without the preservation of associated microfossils, a precise paleosalinity designation remains elusive.

5.5 Carbonate Sand Facies

Based on the available radiocarbon results, the current sedimentary environment initiated around 2600 Cal yrs BP. Two sedimentary layers were associated with this facies, an occasional thin white sand layer and a grey carbonate sand layer. Overall, this facies had a bulk organic matter content of 18.53%. The average coarse fraction content of this layer is 114.5 mg cm^{-3}, which is the coarsest sediment observed in the successions. Microfossils were abundant in the facies, including the ostracodes *Dolerocypria inopinata*, *Hemicytheridea setipunctata, Aurila floridana,* and

Limnocythere floridensis. The following species of foraminifera were also observed: *Ammonia beccarii, Elphidium poeyanum, Elphidium gunteri,* and *Triloculina oblonga* (Fig. 4, 7). The biofacies present in the carbonate sand facies has been termed polyhaline biofacies because the present foraminifera and ostracodes are indicative of more brackish conditions (Dix et al., 1999; Gregory et al., 2015; Teeter, 1995; van Hengstum and Scott, 2012). This unit also included gastropods and bivalves that are common in other Bahamian saline lakes, including *Anomalocardia auberiana*, *Batillaria* sp., *Cerithium* sp.. These species of gastropods and bivalves are associated with brackish-saline shallow water marshes and lagoons (Kjellmark, 1996). No charophytes were present in this layer.

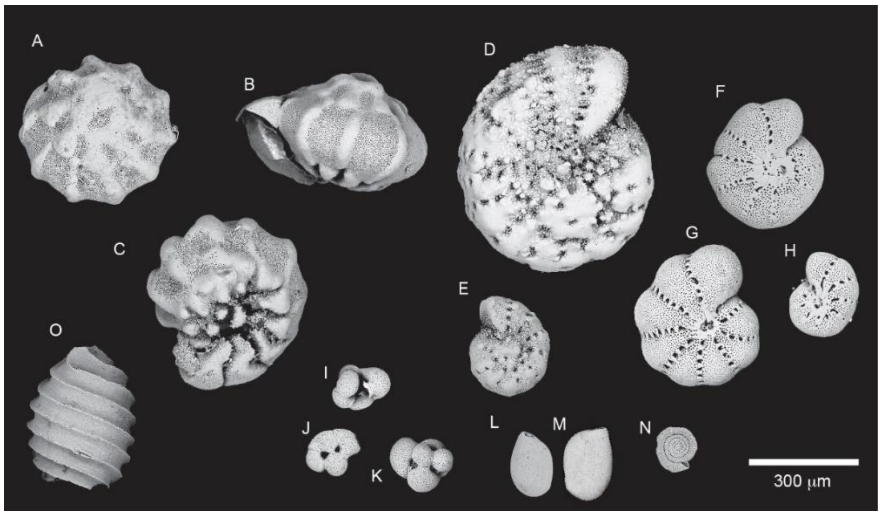

Figure 7. Scanning electron micrographs of foraminifera (A-N) and gyrogonite of a charophyte (O). **A-C:** *Ammonia beccarii* (Linné), **D, E:** *Elphidium gunteri* (Cole), **F-H:** *Elphidium poeyanum* (d'Orbigny), **I-K:** *Helenina davescottensis* van Hengstum, **L, M:** *Triloculina oblonga* (Montagu), **N:** *Spirillina vivipara* (Ehrenberg), **O:** gyrogonite from a charophyte (freshwater to oligohaline macrophyte). All specimens respective to scale bar.

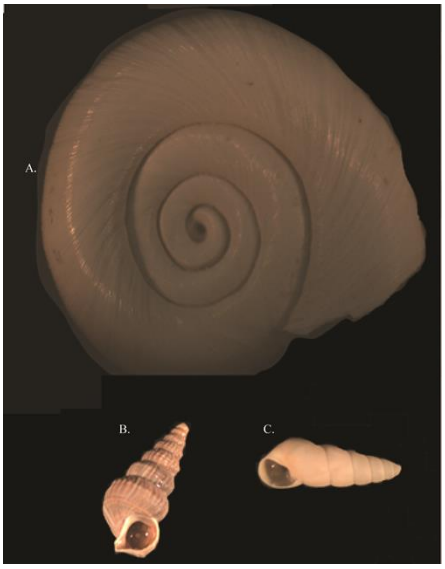

Figure 8. Pictures of some common gastropods found in No Man's Land (A-C). **A:** *Planorbis*, **B:** *Cerithium* sp., **C:** *Hydrobia* sp.

6. DISCUSSION

6.1 Generation of a Oligohaline Constructional Bahamian Lake: 6500 Cal Yrs BP

The basal deposits in the collected successions from No Man's Land sink in Abaco Island was a fragmented granular peat that accumulated prior to 6500 Cal yrs BP. The lack of mangrove propagules or roots or any other marsh vegetation or microfossils suggest that this peat did not accumulate in a marsh environment. In contrast, the peat mostly contained fragments of trees, and had a soil-like appearance. As such, this peat most likely was deposited in a terrestrial environment, which explains the lack of aquatic microfossils. Based on evidence from the northern Bahamas, Holocene sea level was not yet high enough to have flooded the elevation of the peat deposit in No Man's Land (~3-4 m below sea level) by the coastal aquifer (Lighty et al., 1982; Milne and Peros, 2013; Neumann and Land, 1975) (Fig. 5, 9). Given that sea level was ~3-4 meters below present during accumulation of the carbonate mud facies, and that the microfossils indicate the presence of an aquatic environment (see discussion below), No Man's Land must have been functioning as a 'constructional' Bahamian lake at this time. During this period, the balance between regional evaporation and precipitation would have controlled aquatic conditions in No Man's Land.

The carbonate mud facies and co-occurring microfossils in No Man's Land indicate that the basin likely hosted palustrine to lacustrine environmental conditions from 6500 to 4200 years ago, with fresh to slightly brackish conditions. There were three species of ostracodes that dominated the carbonate mud facies: *Candona annae*, *Cypridopsis vidua*, and *Limnocythere floridensis* (Teeter, 1995). *Candona annae* and *Cypridopsis vidua* are both considered to be freshwater ostracodes while *Limnocythere floridensis* prefers more slightly brackish to marine conditions (Teeter, 1980 1995). Gyrogonites of charophytes were also present in this layer, which inhabit fresh and slightly brackish water salinities (Soulié-Märsche, 2008). However, no testate amoeba (van Hengstum et al., 2008) were found in this layer, which means salinity in the basin was likely above 3 psu (van Hengstum et al., 2008). A recently documented species of

foraminifera, *Helenina davescottensis*, was found within this layer in the NML-C4 core (van Hengstum and Bernhard, 2016). In addition, two different morphologies of the carapace of *Limnocythere floridensis* were observed, a 'pointed' variation found only in the carbonate mud facies of NML-C5. This is possibly because there were periods of higher salinity due to less precipitation and more evaporation, which temporarily increased the salinity in the partially aquatic sinkhole. Alternatively, perhaps intervals of increased precipitation favored slightly more fresh conditions that were favorable to charophytes. Based on evidence from elsewhere in the North Atlantic, the Intertropical Convergence Zone (McGee et al., 2014) occupied a more northerly location from 6500 to 4200 Cal yrs (Fig. 9)(Schneider et al., 2014). Given that the ITCZ is associated with atmospheric convection and precipitation, it is likely that a more northerly position of the ITCZ increased regional precipitation in the Northern Bahamas from 6500 to 4200 Cal yrs BP. Another study in Dos Anas Cave in Cuba examined oxygen isotopes in a speleothem that potentially indicates increased precipitation also at this time (Fensterer et al., 2013). There is evidence of large hurricanes in Puerto Rico during this depositional time period (Donnelly and Woodruff, 2007) that may have also supplied greater moisture to the interior of the island. As such, despite the lower position of sea level, and No Man's Land not being flooded by a coastal aquifer, an aquatic environment with low salinity conditions was promoted in No Man's Land, but the microfossils due suggest temporal salinity variations that may have occurred on seasonal or longer timescales.

6.2 Flooding by the Coastal Aquifer at 4200 Cal Yrs BP

The laminated sediments deposited from 4200 to 3300 Cal yrs BP are likely to indicate when laminated microbial mats were present within No Man's Land. Preserved ostracodes indicate that No Man's Land was flooded by saline aquatic conditions. *C. americana,* which typically dominates in Bahamian sinkholes with a salinity greater than 10 psu, but can also tolerate hypersaline conditions (Teeter, 1987). A potential modern analogue for the laminated carbonate mud facies is Storrs Lake on

San Salvador Island or Big Pond on Eluethra Island in the Bahamas. Storr's Lake currently has abundant microbialites, and sediment cores collected from Storrs Lake have a similar laminated stratigraphy as found in No Man's Land from 4200 to 3200 Cal yrs BP. Furthermore, Storrs Lake is currently dominated by the ostracode species *C. americana, and H. setipunctata* (Sipahioglu, 2008). Although *H. setipunctata* was not confidently identified from the Laminated Carbonate Mud Facies, the *Unknown sp. A* does have nearly identical muscle scars as *H. setipunctata* (Fig. 4), perhaps suggesting a possible similar taxonomic affinity. The other possible modern analogue is Big Pond in Eluethera, Bahamas, which also has microbialites and laminated stratigraphy (Glunk et al., 2011).

Based on regional evidence, concomitant vertical migration of the coastal aquifer and Holocene sea-level rise likely flooded No Man's Land at 4200 Cal yrs BP (Lighty et al., 1982; Milne and Peros, 2013; Schneider et al., 2014). The top of the peat deposit is located approximately 4 m below the modern water table level (Fig. 9A) at the position of NML-C5 (Fig. 2). In an extensive stratigraphic analysis the stratigraphy between Abaco and Grand Bahamas Island (Neumann and Land, 1975; Rasmussen and Neumann, 1988), the flooding of the inherited topography by a rising meteoric lens closely followed numerical estimates of regional sea-level rise (Fig. 9A). Assuming the paleo groundwater table was approximately equivalent to the position of sea level at 4200 Cal yrs BP, the uppermost part of the coastal aquifer (van Hengstum and Scott, 2012) should have flooded No Man's Land ~4200 Cal yrs BP (Fig. 9). However, the lack of freshwater microfossils and microbialites that are currently found in saline lakes on lower-latitude Bahamian islands suggests that the water initially flooding No Man's Land was saline. Literature evidence suggests that the ITCZ moved southwards at ~4200 Cal yrs BP (Schneider et al., 2014) (Fig. 8B), which likely decreased moisture delivery in the northern Bahamas. Moisture delivery from Atlantic hurricanes was also likely depressed at this time from decreased regional hurricane activity (Donnelly and Woodruff, 2007; van Hengstum et al., 2016). Based on (a) evidence for decreased regional recharge and sea-level rise and (b) assuming the groundwater table was

approximately equivalent to the position of sea level at 4200 Cal yrs BP, the conditions of the meteoric lens of the coastal aquifer that first flooded No Man's Land ~4200 Cal yrs BP was likely saline.

6.3 Lake Anoxia and Regional Drought: 3300-2600 Cal Yrs BP

The algal sapropel unit was deposited from 3300 to 2600 Cal yrs BP, and it contained no microfossils. This suggests that bottom water conditions were anoxic or corrosive to calcareous microfossils (e.g., foraminifera, ostracodes, charophytes). The algal sapropel itself is not diagnostic of a specific salinity régime, as both Mangrove Lake in Bermuda (marine salinities, anoxic) and Kemp's Bay Bluehole on Andros Island (7-8 psu, oxic) are currently accumulating sapropels sediment. Regional evidence suggests that the southern migration of the ITCZ created an extremely arid time period in the Caribbean from 3300 to 2600 Cal yrs BP. The speleothem from Dos Anas Cave in Cuba exhibited a growth hiatus during these years, which may be driven by stochastic process, but the growth hiatus could also have been driven by decreased regional precipitation (Fensterer et al., 2013). In Playa Bailen lagoon in Cuba, gypsum crystals formed and no lagoonal foraminifera were present at this time (Fig. 9G). In Punta de Cartes, Cuba, few lagoonal foraminifera were found. Both of these events are indicators for a regional dry period (Fig. 9H) (Gregory et al., 2015). From Church's Bluehole on Andros Island, pollen grains in sediment cores indicate an abundance of arid tolerant shrubs at this time (Fig. 9I)(Kjellmark, 1996). In a pollen study from Abaco Island, Slayton (2010) documented a period of grass expansion in the island landscape at this time that may also be a response to regional aridity (Fig. 9J). There was also a noticeable lack of hurricanes occurring in this time period, based on studies in Puerto Rico and in Blackwood sinkhole on Abaco Island (Donnelly and Woodruff, 2007; van Hengstum et al., 2016). The lack of hurricanes reduced the amount of mixing at the site and promoted a stratified water column. The combined regional evidence indicates that aridity in the northern Caribbean from 3300 to 2600 years ago likely promoted anoxic conditions in No Man's Land. However, it remains unknown based on the available data whether the

site was flooded by stratified groundwater with a halocline flooding the benthos, or completely anoxic marine water from 3300 to 2600 Cal yrs BP. However, the lack of any freshwater microfossils in the core would give support to the latter.

6.4 Onset of Modern Conditions: 2600 Cal Yrs BP to Present

The most recent stratigraphic horizon began accumulating 2600 years ago (Figs. 3, 9). It is a carbonate sand facies with ostracodes and foraminifera indicative of more polyhaline conditions (Teeter, 1980; Teeter, 1995). Hurricane activity on Abaco Island increases again as the ITCZ starts to migrate northward at 2600 Cal yrs BP. Based on Caribbean paleoenvironmental records, a final hydroclimate change occurred at 1000 Cal yrs BP (Fensterer et al., 2013; Gregory et al., 2015; Slayton, 2010b). However, No Man's Land did not experience regional changes documented in other locations throughout the Caribbean in the last two millennia. Although the merdional position of the ITCZ became displaced during this time, shoreline migration related to Holocene sea-level rise was likely placed the local mixing zone proximal to the research site, which has created a polyhaline environment. As such, No Man's Land is likely no longer sensitive to climate changes that have occurred in the last 2600 years that may have impacted hydrology in regional meteoric lens.

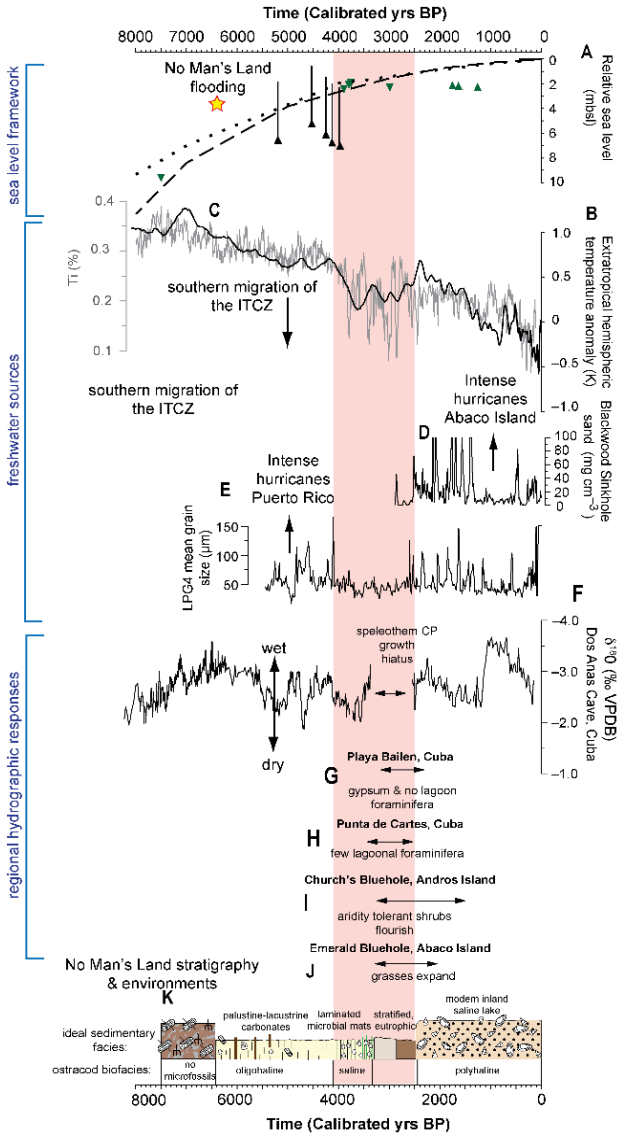

Figure 9. Paleoenvironmental reconstruction of the Northern Caribbean. **(A)** Sea level framework: peat-based maximum sea-level indicators (dark green triangles, Neumann and Land, 1975, Kovacs et al., 2013) and *Acropora* coral minimum sea-level indicators (Lighty et al., 1982, as recalibrated by Milne and Peros, 2013). Also shown are model results from ICE-5G with upper mantle viscosity (UMV) = 5 x 10^{21} Pas and lower mantle viscosity (LMV) of 5 x 10^{22} Pas (Dotted line) and EUST3 with an UMV = 2 x 10^{21} Pas and LMV = 5 x 10^{22} Pas (after Milne and Person, 2013). Freshwater sources: **(B)** temperature contrast between the extratropics of the northern and southern hemispheres (Schneider et al. 2014), **(C)** Ti% from Amazon river output near the Cariaco Basin (Haug et al., 2001), **(D)** evidence for intense hurricane activity in Abaco Island (van Hengstum et al., 2016)), **(E)** evidence for intense hurricane activity in Puerto Rico (Donnelly and Woodruff, 2007). Regional Hydrographic Response: **(F)** precipitation variability in Cuba inferred from the stable oxygen isotopic composition of a speleothem from Cuba (Fensterer et al., 2013), **(G, H)** inferred aridity from lagoonal deposits in Cuba (Gregory et al., 2015), **(I)** Pollen reconstruction showing aridity tolerant shrubs(Kjellmark, 1996), **(J)** Pollen reconstruction showing grass dominance in Emerald Pond in the Bahamas (Slayton, 2010), **(K)** Ideal stratigraphic column from No Man's Land formatted with respect to time (this study).

7. CONCLUSION

A detailed paleoenvironmental reconstruction of No Man's Land Sink in the Bahamas indicates that sea-level rise and ITCZ migrations were the two major ocean and atmospheric forces that drove environmental conditions in No Man's Land Sink over the last 6500 years. The site was a terrestrial environment prior to 6500 Cal yrs BP, and thereafter became a palustrine to lacustrine environment from 6500 to 4200 Cal yrs BP. However, it first became an aquatic environment because a more northerly ITCZ position increased regional precipitation, not sea-level rise, and No Man's Lake functioned as a 'constructional inland lake' at this time (Boush et al., 2014). Eventually concomitant sea-level and groundwater level rise would have flooded No Man's Land with the local coastal aquifer, which appears to have occurred at 4200 Cal yrs BP, based on the core recovery depths and extrapolation from regional sea level curves (Fig. 9). From 4200 to 3300 Cal yrs BP, microbialites living in No Man's Lake deposited a laminated carbonate mud facies dominated by *C. americana*, similar to the modern hypersaline Storrs Lake on San Salvador Island in the Bahamas. Despite the higher position of sea level, elevated salinity conditions could have been maintained by a more southerly position of the ITCZ from 4200 to 2600 Cal yrs, which would have decreased regional rainfall. From 3300 to 2600 Cal yrs BP, the aquatic conditions were perhaps anoxic and saline from regional aridity and drought on Abaco Island. At 2600 Cal yrs BP, a more northern position of the ITCZ promoted increased intense hurricane activity along the western North Atlantic margin and regional precipitation increased, which likely promoted the final transition to accumulation of the modern carbon sand facies in No Man's Land. However, continued shoreline migration with Holocene sea-level rise moved the subsurface mixing zone proximal to No Man's Land Sink, thus desensitizing the site to known regional precipitation changes during the late Holocene.

REFERENCES

Alonso-Zarza, A.M., Tanner, L.H., 2009. Carbonates in continental settings: facies, environments, and processes. Earth Science 61.

Beddows, P.A., Smart, P.L., Whitaker, F.F., Smith, S.L., 2007. Decoupled fresh–saline groundwater circulation of a coastal carbonate aquifer: spatial patterns of temperature and specific electrical conductivity. Journal of Hydrology 346, 18-32.

Boush, L.E.P., Myrbo, A., Michelson, A., 2014. A qualitative and quantitative model for climate-driven lake formation on carbonate platforms based on examples from the Bahamian archipelago. Carbonates and Evaporites 29, 409-418.

Correll, D.S., 1979. The Bahama Archipelago and Its Plant Communities. Taxon 28, 35-40.

Crotty, K., Teeter, J., 1984. Post Pleistocene salinity variations in a blue hole, San Salvador Island, Bahamas, as interpreted from the ostracode fauna, in: Teeter, J.W. (Ed.), Proceedings of The Second Symposium On The Geology of The Bahamas, 3-16.

Dean Jr, W.E., 1974. Determination of carbonate and organic matter in calcareous sediments and sedimentary rocks by loss on ignition: comparison with other methods. Journal of Sedimentary Research 44, 242-248.

Dix, G.R., Patterson, R.T., Park, L.E., 1999. Marine saline ponds as sedimentary archives of late Holocene climate and sea-level variation along a carbonate platform margin: Lee Stocking Island, Bahamas. Palaeogeography, Palaeoclimatology, Palaeoecology 150, 223-246.

Donnelly, J.P., Woodruff, J.D., 2007. Intense hurricane activity over the past 5,000 years controlled by El Niño and the West African monsoon. Nature 447, 465-468.

Fensterer, C., Scholz, D., Hoffmann, D.L., Spötl, C., Schröder-Ritzrau, A., Horn, C., Pajón, J.M., Mangini, A., 2013. Millennial-scale climate variability during the last 12.5 ka recorded in a Caribbean speleothem. Earth and Planetary Science Letters 361, 143-151.

Furtos, N.C., 1936. Fresh-water ostracoda from Florida and North Carolina. American Midland Naturalist 17, 491-522.

Glunk, C., Dupraz, C., Braissant, O., Gallagher, K.L., Verrecchia, E.P., Visscher, P.T., 2011. Microbially mediated carbonate precipitation in a hypersaline lake, Big Pond (Eleuthera, Bahamas). Sedimentology 58, 720-736.

Gregory, B.R.B., Peros, M., Reinhardt, E.G., Donnelly, J.P., 2015. Middle–late Holocene Caribbean aridity inferred from foraminifera and elemental data in sediment cores from two Cuban lagoons. Palaeogeography, Palaeoclimatology, Palaeoecology 426, 229-241.

Hastings, A.K., Krigbaum, J., Steadman, D.W., Albury, N.A., 2014. Domination by reptiles in a terrestrial food web of the Bahamas prior to human occupation. Journal of Herpetology 48, 380-388.

Haug, G.H., Hughen, K.A., Sigman, D.M., Peterson, L.C., Röhl, U., 2001. Southward migration of the intertropical convergence zone through the Holocene. Science 293, 1304-1308.

Heiri, O., Lotter, A.F., Lemcke, G., 2001. Loss on ignition as a method for estimating organic and carbonate content in sediments: reproducibility and comparability of results. Journal of Paleolimnology 25, 101-110.

Hodell, D.A., Curtis, J.H., Jones, G.A., Higuera-Gundy, A., Brenner, M., Binford, M.W., Dorsey, K.T., 1991. Reconstruction of Caribbean climate change over the past 10,500 years. Nature 352, 790-793.

Jury, M., Malmgren, B.A., Winter, A., 2007. Subregional precipitation climate of the Caribbean and relationships with ENSO and NAO. Journal of Geophysical Research: Atmospheres 112, 11.

Kjellmark, E., 1996. Late Holocene climate change and human disturbance on Andros Island, Bahamas. Journal of Paleolimnology 15, 133-145.

Kovacs, S.E., van Hengstum, P.J., Reinhardt, E.G., Donnelly, J.P., Albury, N.A., 2013. Late Holocene sedimentation and hydrologic development in a shallow coastal sinkhole on Great Abaco Island, The Bahamas. Quaternary International 317, 118-132.

Krutak, P.R., 1971. The Recent Ostracoda of Laguna Mandinga, Veracruz, Mexico. Micropaleontology, 1-30.

Lighty, R.G., Macintyre, I.G., Stuckenrath, R., 1982. Acropora palmata reef framework: a reliable indicator of sea level in the western Atlantic for the past 10,000 years. Coral Reefs 1, 125-130.

Linsley, B.K., Dunbar, R.B., Wellington, G.M., Mucciarone, D.A., 1994a. A coral-based reconstruction of Intertropical Convergence Zone variability over Central America since 1707. Journal of Geophysical Research-All Series- 99, 9977-9977.

Linsley, B.K., Dunbar, R.B., Wellington, G.M., Mucciarone, D.A., 1994b. A coral-based reconstruction of Intertropical Convergence Zone variability over Central America since 1707. A Journal of Physical Research: Oceans 99, 9977-9994.

McGee, D., Donohoe, A., Marshall, J., Ferreira, D., 2014. Changes in ITCZ location and cross-equatorial heat transport at the Last Glacial Maximum, Heinrich Stadial 1, and the mid-Holocene. Earth and Planetary Science Letters 390, 69-79.

Michelson, A.V., 2012. Ecological, Taphonomic, and Paleoecological Dynamics of an Ostracode Metacommunity. The University of Akron.

Milne, G.A., Peros, M., 2013. Data–model comparison of Holocene sea-level change in the circum-Caribbean region. Global and Planetary Change 107, 119-131.

Mullins, H.T., Lynts, G.W., 1977. Origin of the northwestern Bahama Platform: review and reinterpretation. Geological Society of America Bulletin 88, 1447-1461.

Mylroie, J.E., Carew, J.L., Moore, A.I., 1995. Blue holes: definition and genesis. Carbonates and Evaporites 10, 225-233.

Neumann, A.C., Land, L.S., 1975. Lime mud deposition and calcareous algae in the Bight of Abaco, Bahamas: a budget. Journal of Sedimentary Research 45, 763-768.

Orem, W.H., Hatcher, P.G., Spiker, E.C., Szeverenyi, N.M., Maciel, G.E., 1986. Dissolved organic matter in anoxic pore waters from Mangrove Lake, Bermuda. Geochimica et Cosmochimica Acta 50, 609-618.

Pérez, L., Lorenschat, J., Brenner, M., Scharf, B., Schwalb, A., 2010. Extant freshwater ostracodes (Crustacea: Ostracoda) from Lago peten itza, Guatemala. Revista de Biología Tropical 58, 871-895.

Peros, M.C., Reinhardt, E.G., Davis, A.M., 2007. A 6000-year record of ecological and hydrological changes from Laguna de la Leche, north coastal Cuba. Quaternary Research 67, 69-82.

Quinn, R., Bull, J., Dix, J., 1998. Optimal processing of marine high-resolution seismic r eflection (Chirp) data. Marine Geophysical Researches 20, 13-20.

Rasmussen, K.A., Neumann, A.C., 1988. Holocene overprints of Pleistocene paleokarst: bight of Abaco, Bahamas, in: James Noel, P.C. (Ed.), Paleokarst. Springer, 132-148.

Reimer, P.J., Bard, E., Bayliss, A., Beck, J.W., Blackwell, P.G., Bronk Ramsey, C., Buck, C.E., Cheng, H., Edwards, R.L., Friedrich, M., Grootes, P.M., Guilderson, T.P., Haflidason, H., Hajdas, I., Hatte, C., Heaton, T.J., Hoffman, D.L., Hogg, A.G., Hughen, K.A., Kaiser, K.F., Kromer, B., Manning, S.W., Niu, M., Reimer, R.W., Richards, D.A., Scott, E.M., Southon, J.R., Stafford, R.A., Turney, C.S.M., van der Plicht, J., 2013. IntCal13 and Marine13 radiocarbon age calibration curves 0-50,000 years Cal BP. Radiocarbon 55, 1869-1887.

Richards, D.A., Smart, P.L., Edwards, R.L., 1994. Maximum sea levels for the last glacial period from U-series ages of submerged speleothems. Nature 367, 357-360.

Schneider, T., Bischoff, T., Haug, G.H., 2014. Migrations and dynamics of the intertropical convergence zone. Nature 513, 45-53.

Schnurrenberger, D., Russell, J., Kelts, K., 2003. Classification of lacustrine sediments based on sedimentary components. Journal of Paleolimnology 29, 141-154.

Sipahioglu, S.M., 2008. Tracking storms through time: event deposition and biologic response in Storr's Lake, San Salvador Island, Bahamas. The University of Akron.

Slayton, I. A. (2010). A vegetation history from Emerald Pond, Great Abaco Island, the Bahamas, based on pollen analysis. (Master of Science), University of Tennessee-Knoxville.

Soulié-Märsche, I., 2008. Charophytes, indicators for low salinity phases in North African sebkhet. Journal of African Earth Sciences 51, 69-76.

Teeter, J., 1980. Ostracoda of the Lake Flirt formation (Pleistocene) of southern Florida. Micropaleontology, 337-355.

Teeter, J.W., 1989. Holocene salinity history of the saline lakes of San Salvador Island, Bahamas. Pleistocene and Holocene Carbonate Environments on San Salvador Island, Bahamas: San Salvador Island, Bahamas, July 2-7, 1989, 35-39.

Teeter, J.W., 1995. Holocene saline lake history, San Salvador Island, Bahamas. Special Papers Geological Society Of America, 117-124.

van Hengstum, P., Reinhardt, E., Beddows, P., Huang, R., Gabriel, J., 2008. Thecamoebians (testate amoebae) and foraminifera from three anchialine cenotes in Mexico: low salinity (1.5–4.5 psu) faunal transitions. The Journal Of Foraminiferal Research 38, 305-317.

van Hengstum, P.J., Bernhard, J.M., 2016. A New Species of Benthic Foraminifera from an Inland Bahamian Carbonate Marsh. The Journal of Foraminiferal Research 46, 193-200.

van Hengstum, P.J., Donnelly, J.P., Fall, P.L., Toomey, M.R., Albury, N.A., Kakuk, B., 2016. The intertropical convergence zone modulates intense hurricane strikes on the western North Atlantic margin. Scientific Reports 6, 21728.

van Hengstum, P.J., Scott, D.B., 2012. Sea-level rise and coastal circulation controlled Holocene groundwater development in Bermuda and caused a meteoric lens to collapse 1600years ago. Marine Micropaleontology 90, 29-43.

van Hengstum, P.J., Scott, D.B., Gröcke, D.R., Charette, M.A., 2011. Sea level controls sedimentation and environments in coastal caves and sinkholes. Marine Geology 286, 35-50.

Zarikian, C.A.A., Swart, P.K., Gifford, J.A., Blackwelder, P.L., 2005. Holocene paleohydrology of Little Salt Spring, Florida, based on ostracod assemblages and stable isotopes. Palaeogeography, Palaeoclimatology, Palaeoecology 225, 134-156.

APPENDIX A

Core photos from NML-C4 and NML-C5